NIH Public Access
Author Manuscript
Audiol Neurootol. Author manuscript; available in PMC 2013 July 18.

Published in final edited form as:
Audiol Neurootol. 2012 ; 17(5): 338–348. doi:10.1159/000339653.

The Effect of Superior Semicircular Canal Dehiscence on Intracochlear Sound Pressures

Dominic V. Pisano[b], **Marlien E.F. Niesten**[a,d], **Saumil N. Merchant**[a,b,c], and **Hideko Heidi Nakajima**[a,b,c,*]

[a]Department of Otology and Laryngology, Harvard Medical School, Boston, MA 02115, USA [b]Eaton-Peabody Laboratory, Massachusetts Eye and Ear Infirmary, 243 Charles St., Boston, MA 02114, USA [c]Speech and Hearing Bioscience & Technology Program, Harvard-MIT Division of Health Sciences & Technology, Cambridge, MA 02139, USA [d]Department of Otorhinolaryngology – Head and Neck Surgery, University medical Center, Utrecht, the Netherlands

Abstract

Semicircular canal dehiscence (SCD) is a pathological opening in the bony wall of the inner ear that can result in conductive hearing loss. The hearing loss is variable across patients, and the precise mechanism and source of variability are not fully understood. Simultaneous measurements of basal intracochlear sound pressures in scala vestibuli (SV) and scala tympani (ST) enable quantification of the differential pressure across the cochlear partition, the stimulus that excites the cochlear partition. We used intracochlear sound pressure measurements in cadaveric preparations to study the effects of SCD size. Sound-induced pressures in SV and ST, as well as stapes velocity and ear-canal pressure were measured simultaneously for various sizes of SCD followed by SCD patching. Our results showed that at low frequencies (<600 Hz), SCD decreased the pressure in both SV and ST, as well as differential pressure, and these effects became more pronounced as dehiscence size was increased. Near 100 Hz, SV decreased about 10 dB for a 0.5 mm dehiscence and 20 dB for a 2 mm dehiscence, while ST decreased about 8 dB for a 0.5 mm dehiscence and 18 dB for a 2mm dehiscence. Differential pressure decreased about 10 dB for a 0.5 mm dehiscence and about 20 dB for a 2 mm dehiscense at 100 Hz. In some ears, for frequencies above 1 kHz, the smallest pinpoint dehiscence had bigger effects on the differential pressure (10 dB decrease) than larger dehiscenses (less than 10 dB decrease), suggesting larger hearing losses in this frequency range. These effects due to SCD were reversible by patching the dehiscence. We also showed that under certain circumstances such as SCD, stapes velocity is not related to how the ear can transduce sound across the cochlear partition because it is not directly related to the differential pressure, emphasizing that certain pathologies cannot be fully assessed by measurements such as stapes velocity.

Keywords

superior semicircular canal dehiscence; cochlear pressure; SCD; scala vestibuli; scala tympani; cochlea; differential pressure

[*]Corresponding author: Heidi Nakajima, EPL, Mass. Eye & Ear Infirm., 243 Charles St., Boston, MA 02114 USA, Tel.: +1 617 573 6954; Fax: +1 617 720 4408, heidi_nakajima@meei.harvard.edu.

NIH-PA Author Manuscript
NIH-PA Author Manuscript
NIH-PA Author Manuscript

NIH-PA Author Manuscript

NIH-PA Author Manuscript

NIH-PA Author Manuscript

INTRODUCTION

Simultaneous measurement of basal intracochlear pressures in scala vestibuli (P_{SV}) and scala tympani (P_{ST}) in human cadaveric temporal bones enables determination of the differential pressure across the cochlear partition. Differential pressure is the stimulus that excites the partition [Nakajima et al., 2009; Voss et al., 1996; Wever and Lawrence, 1950]. We use intracochlear pressure measurements to study superior semicircular canal dehiscence (SCD), an additional opening in the bony wall of the inner ear that does not exist in normal ears. This pathological third window provides an alternative path through which the stimulus-induced fluid displacement of the oval window can flow. SCD can result in conductive hearing loss, but the precise mechanism is presently not well understood.

It has been demonstrated previously that the induction of SCDs in chinchillas [Songer and Rosowski, 2006] and human temporal bones [Chien et al., 2007] produces sound-induced motion of the lymph in the semicircular canal and results in increases in ossicular velocity at frequencies less than 1 kHz. It has also been demonstrated in chinchilla that SCDs produce decreases in the low-frequency sound-induced cochlear potentials measured near the round window in response to wide-band chirps [Songer and Rosowski, 2005]. These results have led to the suggestion that SCD acts to reduce the sound pressure in the cochlear vestibule as well as the sound pressure difference across the cochlear partition [Songer and Rosowski, 2007]. The present study presents a test of those hypotheses via direct measurements of the sound pressures in scala vestibuli and tympani of human cadaveric temporal bone preparations before and after induced SCDs. These direct measurements of the mechanical consequences of SCD on the hearing process also help shed light on why the severity of hearing loss varies among individuals with SCD.

A subset of the results presented here was the subject of a presentation at the 2011 Mechanics of Hearing Meeting, and was included in a proceedings manuscript [Nakajima et al., 2011].

METHODS

Temporal Bone Preparation

Temporal bones were removed by an intracranial approach [Nadol, 1996] during autopsy within 24 hours of death, after permission was granted to obtain specimens for research. Immediately after removal, the specimens were stored in 0.9% normal saline and refrigerated. Only a brief description of our temporal bone preparation is presented here as details are available in Nakajima et al. [2009]. The bony ear canal was shortened to a length of about 1 cm, a mastoidectomy performed and the facial recess opened widely for middle- and inner-ear access. The stapedial tendon was removed to allow access to the area surrounding the oval window. The promontory was thinned near the oval and round windows where the pressure sensors were to be inserted. The epitympanic region was opened to access the superior semicircular canal from the lateral transmastoid approach. A 2-3 mm length of the bone overlying the superior semicircular canal near the arcuate eminence was thinned where the superior semicircular canal is adjacent to the temporal lobe of the middle fossa.

The temporal bone was positioned such that the tympanic ring of the tympanic membrane was roughly horizontal. This position allowed for easy immersion of the inner-ear compartment in saline during the cochleostomy procedure and during the opening of the dehiscence. To seal the pressure transducers in the cochleostomies, the fluid around the inner ear was lowered so that a meniscus of saline surrounded the cochleostomy and the

NIH-PA Author Manuscript

NIH-PA Author Manuscript

NIH-PA Author Manuscript

inserted transducer; then Jeltrate ® dental impression material was applied. This procedure ensured that air was not introduced into the cochlea.

The transmastoid (lateral) approach for the SCD was chosen to enable the dehiscence to remain immersed in saline throughout the preparation and measurement procedure. The region of the superior semicircular canal dehiscences was kept slightly lower than the area where stapes velocity measurements were made (thus the SCD dehiscence always had about 1mm fluid above the hole and the posterior crus of the stapes was above fluid). The SCDs were made facing laterally (transmastoid approach), enabling the same general direction of the SCD opening as the cochleostomy openings for the pressure sensors. There are likely no differences in intracochlear pressure effects between slight directional differences of the dehiscence (about 90 degree difference, facing laterally versus superiorly along the same section of the semicircular canal arc). Because our goal in this study was to determine whether hole size affected hearing – as long as parameters except size were generally kept consistent, and the effects were reversible – our goal was reached.

Sound Stimulation, Ear Canal Pressure, Ossicular Velocity

Sound stimuli, velocity measurements and pressure recordings were performed in the manner described by Nakajima et al. [2009] and illustrated in Fig. 1. Sound stimulation was presented to the sealed ear canal via an earphone (Radio Shack 40-1377) coupled to the canal with flexible tubing. Ear-canal sound pressure (P_{EC}) was recorded with a calibrated probe tube microphone (Etymotic ER-7C) with the tip of the flexible probe tube positioned approximately 1-2 mm from the umbo of the tympanic membrane. Velocities for Stapes (V_{Stap}) and round window were measured with a laser Doppler vibrometer (Polytec CLV700) aimed at 0.2 mm^2 reflectors (consisting of polystyrene micro beads) placed on the posterior crus of the stapes and the round window membrane. All measured velocities were referenced by the simultaneously measured P_{EC} and are reported as such with units of $m\text{-}s^{-1}\text{-}Pa^{-1}$. Phase comparison between V_{Stap} and round-window velocity was made to ensure a ½ cycle difference below 500 Hz; such a phase difference indicates that air was not introduced into the inner ear and that a pre-existing third window was not present.

Pressure Sensors

Intracochlear sound pressures were measured in scala vestibuli (P_{SV}) and scala tympani (P_{ST}) simultaneously with micro-optical pressure sensors developed by Olson [1998], along with P_{EC} and V_{Stap}. Figure 1 illustrates the various measurements made. The pressure sensors were inserted through (~ 200 μm diameter) cochleostomies drilled in the bony promontory into scala vestibuli and tympani [Nakajima et al., 2009]. The sensors were placed approximately 100-200 μm deep into the scalae. During drilling and sensor insertion, the regions surrounding the cochleostomies were immersed in saline. The sensors were sealed to the surrounding cochlear bone with dental alginate impression material (Jeltrate, L.D. Caulk Co.) to prevent release of fluid from the cochlea, and to prevent air leaking into the cochlea. Repeated calibrations of the sensitivity of the pressure sensors [Olson, 1998; Nakajima et al., 2009] were performed just before intracochlear placement and after removal of the sensors from the cochlea. The similarity of the calibrations made before placement and after removal of the sensors (differences of less than 2 dB) was an important constraint on the quality of our results.

SCD

The superior semicircular canal was accessed by the lateral transmastoid approach where various sizes of dehiscences (from small to large) were made consistently near the arcuate eminence interfacing the middle cranial fossa. CT scans of the temporal bones after the experiment showed that the location (center of the SCD along the arc of the superior

NIH-PA Author Manuscript

NIH-PA Author Manuscript

NIH-PA Author Manuscript

semicircular canal) varied approximately between 4 – 5 mm from the ampulla. Starting with a pinpoint hole of approximately 0.5 mm diameter, the dehiscence was enlarged in length to 1 mm and then 2 mm with constant widths of approximately 0.5 mm. Simultaneous recordings of P_{SV} and P_{ST}, as well as V_{Stap} and P_{EC} were made before and after each increase in dehiscence size. We then attempted to reverse the effects of the SCD by patching the dehiscence with dental impression material or dental cement.

Generally, dental impression material placed over the dehiscence reversed the effect of the SCD on V_{Stap}, P_{SV}, and P_{ST}. Dental cement was less effective. It is possible that the dental impression material (which is water soluble before drying) sealed the hole completely, while the dental cement, which requires a dry substrate, did not always completely seal the dehiscence.

Summary of Specimens Used

Summary of the specimens used are shown in Table I. Experiments were conducted on twenty five human temporal bones for this study. The first three bones were used to develop techniques. In nine bones, complications occurred such as: air introduced into the inner ear, abnormally low middle-ear motion, or trauma to the preparation. In three bones, both scala vestibuli and scala tympani pressure sensors became unstable (i.e. calibration at the end of the experiment differed from the beginning by over 2 dB). Of the remaining ten temporal bones, six ears provided P_{SV} results with stable sensors (five with reversal of SCD effect after patching, and one with incomplete reversal), eight ears provided P_{ST} results with stable sensors (six with reversal of SCD effect after patching, and two with incomplete reversal), and three ears had both P_{SV} and P_{ST} sensors that were stable with good reversal of SCD effects.

RESULTS

Stapes Velocity (V_{Stap})

Stapes velocity relative to ear-canal pressure measured before and after creating dehiscences in the superior semicircular canal of various sizes showed that changes in V_{Stap} due to SCD varied across ears. Figure 2 shows three representative examples of V_{Stap} /P_{EC} magnitude and phase for the initial state (black solid lines), after various SCD sizes, and after patching the SCD (black dashed lines). The three examples show variations in the amount and frequency range of the SCD-induced change in V_{Stap} across ears and that these changes were reversible by patching the SCD.

In general, an increase in SCD size resulted in an incremental increase in the magnitude of V_{Stap} over some range of frequencies; however, the frequency range of the effect as well as the amount of change varied across ears. In Fig. 2A, there is a wide frequency range (up to 7 kHz) where there is a monotonic relationship between magnitude and dehiscence size. In contrast, Fig. 2B shows an example where an incremental increase in V_{Stap} with dehiscence size only occurs below 1 kHz, while between 1 to 2 kHz, V_{Stap} magnitude actually decreases as dehiscence size increases. Another example of how dehiscence size can affect V_{Stap} in a complicated manner is shown in Fig. 2C, where only the pinpoint dehiscence (~0.5 mm diameter) resulted in an increase in stapes velocity below 600 Hz. Between 1 to 2 kHz the pin-hole dehiscence actually produced a decrease in V_{Stap} magnitude (instead of an increase as seen in the larger dehiscences). Overall, for dehiscences of approximately 2 mm, V_{Stap} increased in magnitude over varying frequency ranges (below 4 kHz for 4 ears, below 1 kHz for 4 ears, 0.8 to 6 kHz for 2 ears). All 10 ears showed reversal of these increases in V_{Stap} after patching the SCD. SCD induced increases in V_{Stap} has been reported earlier in

NIH-PA Author Manuscript

NIH-PA Author Manuscript

NIH-PA Author Manuscript

temporal bones [Chien et al., 2007] and animal studies [Songer et al., 2006; Rosowski et al., 2004].

The stapes velocity results are generally consistent with the idea that the SCD shunts the fluid flow evoked by oval-window motion, allowing increased freedom of stapes motion due to the decrease in the acoustic impedance of the inner ear. However, the frequency range of these effects varies. Notably, as shown by the representative example in Fig. 2C, the effect of dehiscence size on V_{Stap} can be complicated, especially for smaller dehiscences. This is because V_{Stap} is affected by the overall inner-ear input impedance, including the impedance within the vestibule, the impedances of the individual scalae compartments, as well as the impedance of the dividing cochlear partition. Because of these complexities, V_{Stap} is not always well correlated with the sound pressure across the cochlear partition, and therefore is not a good indicator of how hearing is affected by SCD.

Pressure in Scala Vestibuli (P_{SV})

The effect of SCD on scala vestibuli pressure varied across ears, and generally two types of effects were seen. Figure 3 illustrates representative examples of the two response types. Plotted in the figure is scala vestibuli pressure relative to ear-canal pressure (P_{SV}/P_{EC}) in the initial state (black solid lines), after various SCD sizes, and after patching the SCD (black dashed lines). Figure 3A plots an example of a simple monotonic relationship where P_{SV} magnitude decreased and the phase changed to the leading direction with increase in SCD size for a wide frequency range (<3 kHz). Patching the SCD resulted in reversal of the effects of SCD on P_{SV} in this preparation with stability of the pressure sensor calibration within 2 dB. The trend of incremental decreases in P_{SV} with increases in SCD size was seen in 4 out of 6 ears where the P_{SV} sensors were stable and the SCD effects were reversible in all except one where the SCD was not completely reversed by patching with dental cement.

Figure 3B shows a representative ear showing a more complicated effect of SCD size on P_{SV}/P_{EC}. In the low frequency region (<500 Hz), the magnitude decreased and the phase showed an increased lead as SCD size was increased, similar to the effect seen in 3A. However, for frequencies above 1 kHz, the smallest dehiscence (0.5 mm diameter) yielded the biggest decrease in magnitude (compared to the larger dehiscences) and the phase generally remained the same. The larger dehiscences (1 and 2 mm long) affected the magnitude and phase of P_{SV} in a manner similar to the behavior in the low frequency region and to the example of 3A for all frequencies. The pressure sensor was stable to within 1 dB during the experiment and the effect of SCD was reversible. Two ears out of 6 had this complicated relationship where the smallest pinpoint dehiscence had the largest effect on P_{SV} in the mid-to-high frequencies; both ears had pressure measurements that were reversible after patching the SCD. The ears that had the complicated P_{SV} effect due to the smallest dehiscences, were also the same ears that showed the complicated relationship in the V_{Stap} (as in Fig. 2C) mentioned earlier.

Pressure in Scala Tympani (P_{ST})

As illustrated in representative examples in Fig. 4, SCD had two types of effect on scala tympani pressure relative to ear-canal pressure (P_{ST}/P_{EC}). In both types, increases in SCD size decreased the magnitude and changed the phase to the leading direction for low frequencies (below 400-700 Hz). The difference between the two types of effects occurred in the higher frequencies (above 400-700 Hz). In one type of SCD effect, shown in the representative example of Fig. 4A, P_{ST} at higher frequency did not change significantly (the pressure sensor calibration in this case remained within 1 dB). Four of the 8 P_{ST} data had this simple relationship with SCD size, and the SCD effects were reversible except one ear with the SCD patched with dental cement which did not show complete reversal of the SCD.

NIH-PA Author Manuscript

NIH-PA Author Manuscript

NIH-PA Author Manuscript

In the other type of SCD effect, shown in Fig. 4B, P_{ST} increased in magnitude with increasing size of SCD in the mid-to-high-frequency range (the pressure sensor calibration in this case remained within 1 dB). The phase was either slightly in the leading direction compared to the initial state, or changed little with the SCD. This second type of effect was seen in 4 out of 8 P_{ST} measurements, and all 4 had stable pressure sensors and 3 had reversibility of the SCD effects. Five of the 8 ears with stable P_{ST} pressure sensors also had stable P_{SV} pressure sensors. There did not appear to be a relationship between the type of SCD effect on P_{SV} (Fig. 3 A or B) and the type of effect on P_{ST} (Fig. 4 A or B).

Average Change in Intracochlear Pressures Due to SCD

To illustrate the general effect of SCD, the average change in intracochlear pressure was calculated for scala vestibuli and scala tympani pressures. Figure 5 plots the geometric mean and standard deviation of the magnitude (error bars) and arithmetic mean and standard deviation of the phase for changes in P_{SV} and P_{ST} due to various sizes of SCD (represented by different colors). The averages included five P_{SV} (Fig. 5A) and six P_{ST} (Fig. 5B) measurements, where all of the included experiments exhibited stable pressure sensor calibrations and the reversing of SCD effects by patching. Below 600 Hz, the magnitude of both P_{SV} and P_{ST} monotonically decreased and the phase shifted towards the leading direction with increases in SCD size. These general changes in intracochlear pressures below 600 Hz and their monotonic relationship with SCD size were consistent for all temporal bones. However, across ears, there were variations in the absolute amount of pressure change induced by a given dehiscence size as illustrated by the large error bars. Calculations of correlation coefficients for P_{SV} magnitude showed statistical significance (p-values between 0.002 to 0.01) below 200 Hz with R^2 between 0.41 and 0.52. P_{ST} magnitude also showed statistical significance (p-values between 0.01 to 0.036) below 200 Hz with R^2 between 0.246 and 0.350. The lower R^2 and poor statistical significance at higher frequencies describes a significant variation in the effects of the SCD across ears and also reflects the relatively small sample size in our study.

Differential Pressure Across the Cochlear Partition

The differential pressure ($P_{SV} - P_{ST}$) across the partition of the basal section of the cochlea (where the differences of the real and imaginary parts of the pressures are linearly subtracted) is thought to represent the final acoustic input to the cochlea. Thus, this difference can predict how various pathologies, such as SCD, affect hearing function when the sensory apparatus of the inner ear is unaltered, and we can use our measurements of this difference in our cadaveric preparations to estimate how SCD might affect hearing in live humans.

Representative examples of two types of SCD effects on the differential pressure relative to ear-canal pressure, $(P_{SV} - P_{ST})/P_{EC}$, are illustrated in Figure 6. Both examples illustrate similar low-frequency (below 600-700 Hz) changes with SCD size: differential pressure magnitude decreased and the phase increased monotonically towards the leading direction with increases in SCD size. The mid-to-high frequency changes owing to SCD varied across ears. In one type of SCD effect, shown in Fig. 6A, the differential pressure changed insignificantly for frequencies above ~600 Hz (both P_{SV} and P_{ST} pressure sensors were stable within 1 dB). In the other type of high-frequency SCD effect, shown in Fig. 6B, the smallest pinpoint SCD had the greatest effect: it decreased differential pressure magnitude more than did larger dehiscences, and it altered the phase of the pressure difference in a direction opposite to the changes produced by the larger dehiscences (both P_{SV} and P_{ST} pressure sensors were stable within 1 dB). Only three experiments succeeded in having both pressure sensors in scala vestibuli and scala tympani stable in calibration throughout the experiment, as well as exhibiting full reversal of both P_{SV} and P_{ST} pressures after patching

NIH-PA Author Manuscript

NIH-PA Author Manuscript

NIH-PA Author Manuscript

the SCD. Two ears had the type of SCD effect shown in Fig. 6A, while one ear had the effect shown in Fig. 6B. The ear that had the complicated behavior of differential pressure due to a pinpoint dehiscence (Fig. 6B) also had a similarly complicated behavior in P_{SV} (Fig. 3B). Furthermore, this ear had V_{Stap} that showed more effect due to the pinpoint dehiscence at low frequencies (<1 kHz) (Fig. 2C) than the larger dehiscences.

DISCUSSION

Measurements of intracochlear sound pressures in scala vestibuli and scala tympani in cadaveric temporal bones enabled experimental evaluation of how SCD can affect hearing. The effects of SCD on intracochlear pressures in scala vestibuli and scala tympani were reversible by patching the dehiscence. This ensured that the effects observed were solely due to the various manipulations made at the superior semicircular canal. As discussed in the Methods section, patching the SCD with dental impression material was superior to dental cement, likely due to the impression material enabling a tight fluid seal versus the cement that may have allowed a small leak.

The results showed that both low-frequency (below 400-700 Hz) P_{SV} and P_{ST} magnitudes decreased and their phases shifted to the leading direction due to SCD. For low frequencies (< 600 Hz) the effects on P_{SV} and P_{ST} were more pronounced with an increase in SCD size. This monotonic relationship of magnitudes decreasing and phases increasingly leading with increasing SCD size sometimes held true for all frequencies in P_{SV}. However, for some ears (2/6 ears) at frequencies above 1 kHz, the smaller pinpoint dehiscence (~0.5 mm diameter) produced the largest decreases in P_{SV} magnitude as compared to larger dehiscences. In these same ears, P_{ST} increased with increasing SCD size or had little change for frequencies above 400-700 Hz.

Calculations of the differential pressure across the partition showed that increase in SCD size resulted in decreased differential pressure for frequencies below 600 Hz. This would be interpreted as more conductive hearing loss with increased SCD size for frequencies below 600 Hz. These low-frequency decreases in the differential pressure for an SCD around 2 mm long were between 10-20 dB, similar to the amount of conductive hearing loss seen in patients with SCD of about 2 mm. However, an interesting finding is that above 1 kHz, the smallest pinpoint hole in the superior semicircular canal sometimes resulted in more differential pressure decrease, representing more conductive hearing loss than the larger dehiscence sizes.

When the differential pressure decreased more at frequencies above 1 kHz due to the smallest SCD dehiscence (compared to the larger dehiscences), P_{SV} also had a similar pattern. However, there did not appear to be a correlation with unusual differences in P_{ST} at the higher frequencies. Interestingly, the V_{Stap} response was also unusual, but in a non-predictable manner. Although the low-frequency P_{SV} and P_{ST}, as well as the differential pressure, decreased in a monotonic relationship with SCD size, the V_{Stap} increase was not monotonic with SCD size as might be expected, but instead, the smallest size SCD resulted in the biggest increase in V_{Stap} (Fig. 2C). For the higher frequencies, the smallest dehiscence resulted in the most decrease in P_{SV} and the differential pressure, however instead of an expected V_{Stap} increase (as was seen in the larger dehiscenes), V_{Stap} decreased. V_{Stap} is related to the impedance presented by the whole inner ear at the oval window. Under certain circumstances such as SCD, V_{Stap} is not related to how the ear can transduce sound across the cochlear partition because it is not directly related to the differential pressure. Thus comparisons of V_{Stap} and differential pressure emphasize that inner-ear pathologies, such as third-window effects, cannot be fully assessed by measurements such as V_{Stap}.

NIH-PA Author Manuscript

NIH-PA Author Manuscript

NIH-PA Author Manuscript

The observed non-monotonic effect of SCD size on hearing across frequency may explain why most of the clinical studies trying to correlate the size of SCD to various symptoms have not shown consensus. For example, no correlation between SCD size and air-bone gaps were found in multiple clinical studies [Pfammater et al., 2010; Chi et al., 2010; Martin et al., 2009; Mikulec et al., 2004]. However Yuen et al. [2009] did find correlation between the dehiscence size and low-frequency (500-2000 Hz) air-bone gap in patients with 3 mm or larger SCDs (18 ears).

The approach taken in this study has some limitations in regard to direct comparison with clinical findings. In our experiments, the dehiscence was surrounded by fluid to prevent air from entering the semicircular canal and to keep the static pressure of the fluid at the interface of the dehiscence consistent across the various sizes. In a patient, an SCD would be in contact with cerebral spinal fluid, dura and/or brain. The static pressure at the SCD interface in patients would differ from our experimental condition. Many other variables can differ across patients even if – as determined radiologically – the size and location of the bony dehiscence may be similar; for example, the adherence of the dura to the edges of the dehiscence can vary, and how much the overlying brain and/or dura pushes into the dehiscence can vary. This may explain why some patients with incidental findings of SCD on imaging have no symptoms, and why some patients experience symptoms acutely.

Although the condition surrounding the SCD in our experiment differs slightly from the clinical situation, details regarding the effect of SCD on hearing can be better understood in this present study than in clinical studies, especially because various sizes of SCD can be induced in the same ear without changing other variables, and reversal of the SCD can ensure that the pressures return to the pre-SCD baseline measurements.

The experiments in which the smallest SCD resulted in the largest conductive hearing loss might be explained by the effects of the hole size on resistance to fluid flow through the hole and resulting absorption of acoustic energy. For no hole, there is no shunt connection from the scala vestibuli compartment. For a large hole the sound flow through the dehiscence depends on the shunt impedance that is probably dominated by the inertance associated with flow through the canal remnant as well as the input impedance of the compartment to which fluid flows (Songer and Rosowski 2007). For very small holes, however, the resistance to fluid flow through the opening may become important, and the damping it provides may have a broadband effect on scala vestibuli pressure.

Furthermore, the effect of SCD on V_{Stap} can be complicated and show little relationship to the differential pressure across the partition. Again, this is likely due to the impedance that is presented at the oval window, which can be influenced by various factors such as the balance between the effect of the annular ligament surrounding the stapes footplate in relationship to the impedances of the inner-ear structures. Thus, V_{Stap} may have no simple relationship to the size of the dehiscence, the effect on intracochelar pressures, the differential pressure across the partition, and most importantly no unique relationship to how the ear transduces sound across the cochlear partition. This example demonstrates the importance of understanding the mechanical effect of pathologies on hearing by measuring the differential pressure across the partition, and that measurements such as V_{Stap} do not necessarily determine the effect of pathology on hearing.

Future studies will focus on modeling the inner ear impedances to simulate the effect of SCD in humans to aid in the explanation of these findings. Furthermore, larger sized SCD (larger than 2 mm) occur clinically as do variation in SCD location, thus these parameters will be topics of future study. From model predictions of Songer and Rosowski (2007), it would be expected that the effect of SCD will not continue to increase with increase in SCD

NIH-PA Author Manuscript

NIH-PA Author Manuscript

NIH-PA Author Manuscript

size after exceeding a certain SCD size. Additionally, in some patients, low-frequency hypersensitive bone conduction has been observed (Minor 2000; Minor et al. 2003; Mikulec et al. 2004). Our intracochlear pressure measurements have the potential to illuminate how bone conduction transduces sound to the cochlea. This is a topic that we certainly plan to take up. After learning some of the basics regarding bone conduction mechanism by intracochlear pressure measurments, we plan to study the effect of SCD on bone conduction using our methodology. SCD would be expected to have different effects on the air-conduction and bone-conduction mechanisms that produce the pressure difference across the cochlear partition.

Acknowledgments

John Rosowski kindly provided advice on this project and manuscript. We thank Diane Jones, Mike Ravicz, and Ishmael Stefanov-Wagner and the other staff of the Otolaryngology Department and Eaton Peabody Laboratory for their generous contributions. We are also indebted to Lisa Olson for consulting on our work and providing expertise regarding the fiberoptic micro pressure transducers. This work was carried out in part through the use of MIT's Microsystems Technology Laboratories for the fabrication of the micro fiberoptic pressure sensors. Support was provided by NIH grants R03DC011158 (HHN) and R01DC004798 (SNM).

References

Chi FL, Ren DD, Dai CF. Variety of audiologic manifestations in patients with superior semicircular canal dehiscence. Otol Neurotol. 2010; 31:2–10. [PubMed: 20050265]

Chien W, Ravicz ME, Rosowski JJ, Merchant SN. Measurements of human middle- and inner-ear mechanics with dehiscence of the superior semicircular canal. Otol Neurotol. 2007; 28:250–7. [PubMed: 17255894]

Martin C, Chahine P, Veyret C, Richard C, Prades JM, Pouget JF. Prospective radiological study concerning a series of patients suffering from conductive or mixed hearing loss due to superior semicircular canal dehiscence. Eur Arch Otorhinolaryngol. 2009; 266:1175–1181. [PubMed: 19002698]

Mikulec AA, McKenna MJ, Ramsey MJ, Rosowski JJ, Herrmann BS, Rauch SD, Curtin HD, Merchant SN, Mikulec AA, McKenna MJ, Ramsey MJ, Rosowski JJ, Herrmann BS, Rauch SD, Curtin HD, Merchant SN. Superior semicircular canal dehiscence presenting as conductive hearing loss without vertigo. Otol Neurotol. 2004; 25:121–129. [PubMed: 15021770]

Minor LB. Superior canal dehiscence syndrome. 2000; 21:9–19.

Minor LB, Carey JP, Cremer PD, Lustig LR, Streubel SO, Ruckenstein MJ. Dehiscence of bone overlying the superior canal as a cause of apparent conductive hearing loss. Otol Neurotol. 2003; 24:270–8. [PubMed: 12621343]

Nadol JB. Techniques for human temporal bone removal: Information for the scientific community. Otolaryngol Head Neck Surg. 1996; 115:298–305. [PubMed: 8861882]

Nakajima HH, Dong W, Olson ES, Merchant SN, Ravicz ME, Rosowski JJ. Differential Intracochlear Sound Pressure Measurements in Normal Human Temporal Bones. J Assoc Res Otolaryngol. 2009; 10:23–36. [PubMed: 19067078]

Nakajima, HH.; Pisano, DV.; Merchant, SN.; Rosowski, JJ. The effect of superior semicircular canal dehiscence on intracochlear sound pressures. In: Shera, CA.; Olson, ES., editors. What Fire is in Mine Ears: Progress in Auditory Biomechanics, Proceedings of the 11th International Mechanics of Hearing Workshop. American Institute of Physics; 2011. p. 110-115.

Olson ES. Observing middle and inner ear mechanics with novel intracochlear pressure sensors. J Acoust Soc Am. 1998; 103:3445–3463. [PubMed: 9637031]

Pfammatter A, Darrouzet V, Gärtner M, Somers T, Van Dinther J, Trabalzini F, Ayache D, Linder T. A superior semicircular canal dehiscence syndrome multicenter study: is there an association between size and symptoms? Otol Neurotol. 2010; 31:447–454. [PubMed: 20118818]

Rosowski JJ, Songer JE, Nakajima HH, Brinsko KM, Merchant SN. Clinical, experimental, and theoretical investigations of the effect of superior semicircular canal dehiscence on hearing mechanisms. Otol Neurotol. 2004 May 25.:323–332. [PubMed: 15129113]

NIH-PA Author Manuscript

NIH-PA Author Manuscript

NIH-PA Author Manuscript

Songer JE, Rosowski JJ. The effect of superior canal dehiscence on cochlear potential in response to air-conducted stimuli in chinchilla. Hear Res. 2005; 210:53–62. [PubMed: 16150562]

Songer JE, Rosowski JJ. The effect of superior-canal opening on middle-ear input admittance and air-conducted stapes velocity in chinchilla. J Acoust Soc Am. 2006; 120:258–269. [PubMed: 16875223]

Songer JE, Rosowski JJ. A mechano-acoustic model of the effect of superior canal dehiscence on hearing in chinchilla. J Acoust Soc Am. 2007; 122:943–51. [PubMed: 17672643]

Voss SE, Rosowski JJ, Peake WT. Is the pressure difference between the oval and round windows the effective acoustic stimulus for the cochlea? J Acoust Soc Am. 1996; 100:1602–1616. [PubMed: 8817890]

Wever EG, Lawrence M. The acoustic pathways to the cochlea. J Acout Soc Am. 1950; 22:460–467.

Yuen HW, Boeddinghaus R, Eikelboom RH, Atlas MD. The relationship between the air-bone gap and the size of superior semicircular canal dehiscence. Otolaryngol Head Neck Surg. 2009; 141:689–694. [PubMed: 19932839]

NIH-PA Author Manuscript

NIH-PA Author Manuscript

NIH-PA Author Manuscript

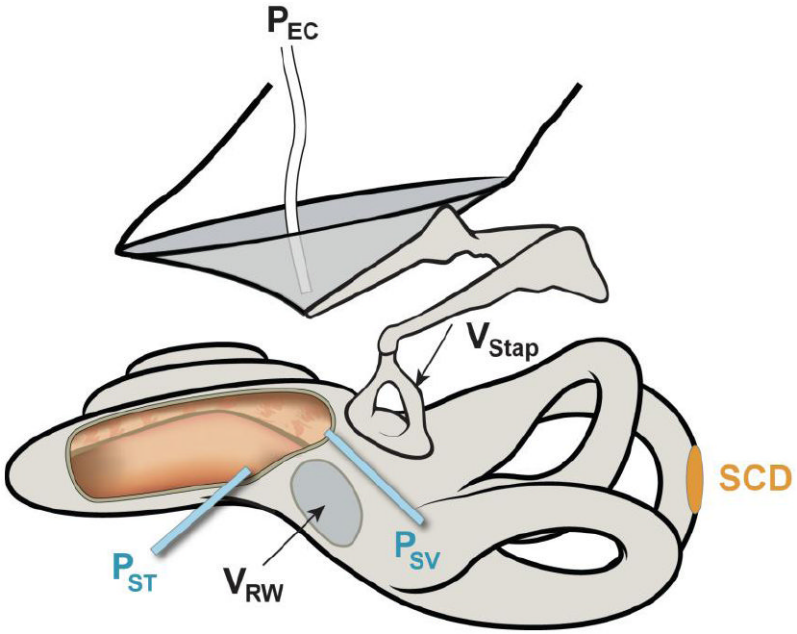

Figure 1.

Illustration of a left ear demonstrating a superior semicircular canal dehiscence (SCD) along with measurements made. Measurements included sound pressure in the ear canal (P_{EC}) with a probe-tube microphone, stapes velocity (V_{Stap}) and round-window velocity (V_{RW}) with laser Doppler vibrometry and sound pressures in scala vestibuli (P_{SV}) and scala tympani (P_{ST}) measured simultaneously with micro-optical pressure transducers. For illustration purposes only, the scalae are shown opened (cut-out area to the left of the round window) to show the placement of the transducers within the two perilymphatic scalae.

NIH-PA Author Manuscript
NIH-PA Author Manuscript
NIH-PA Author Manuscript

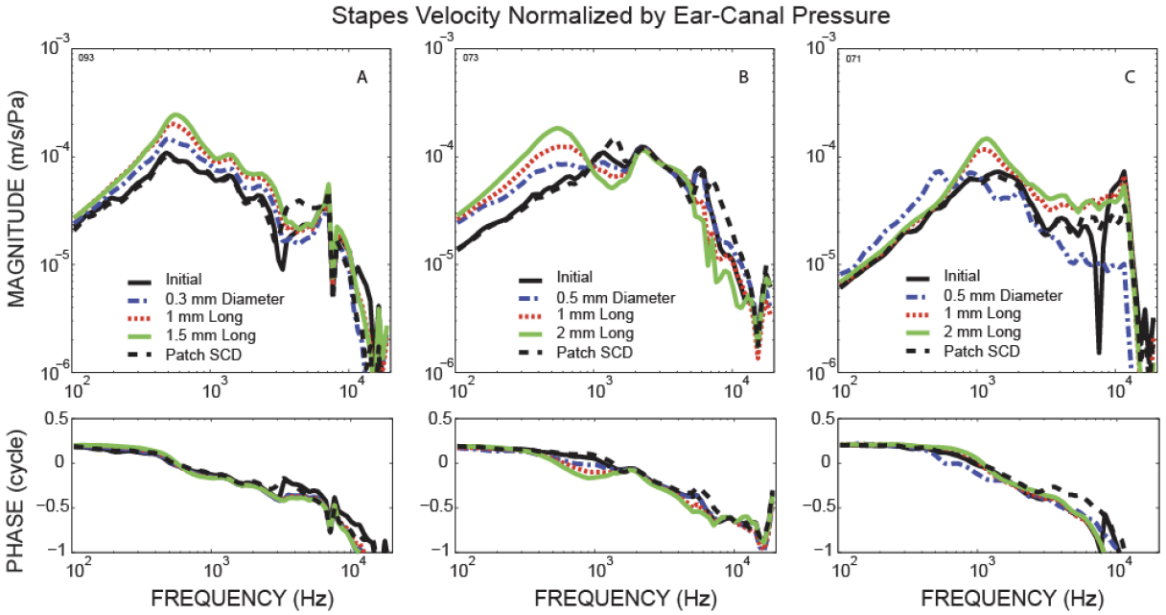

Figure 2.

Three (A, B, C) representative examples of stapes velocity relative to ear-canal pressure including the magnitude and phase for the initial state, after inducing SCD of various sizes, and after patching the SCD.

NIH-PA Author Manuscript
NIH-PA Author Manuscript
NIH-PA Author Manuscript

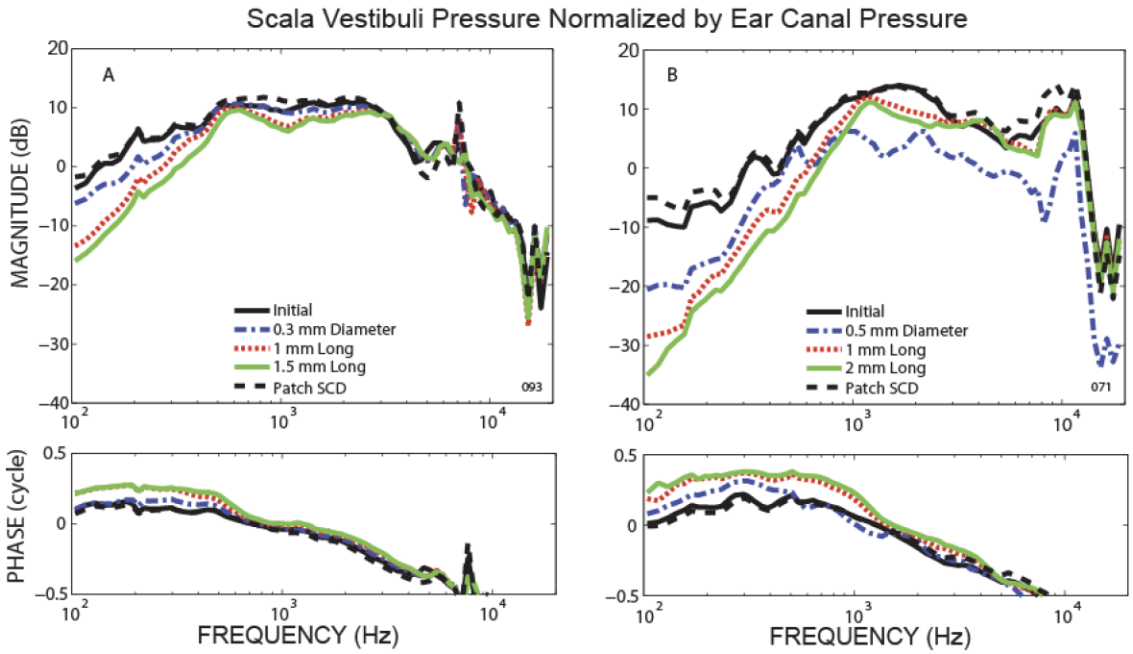

Figure 3.
Representative example of scala vestibuli pressure relative to ear canal pressure for the initial state, after various SCD sizes, and after patching the SCD.

NIH-PA Author Manuscript
NIH-PA Author Manuscript
NIH-PA Author Manuscript

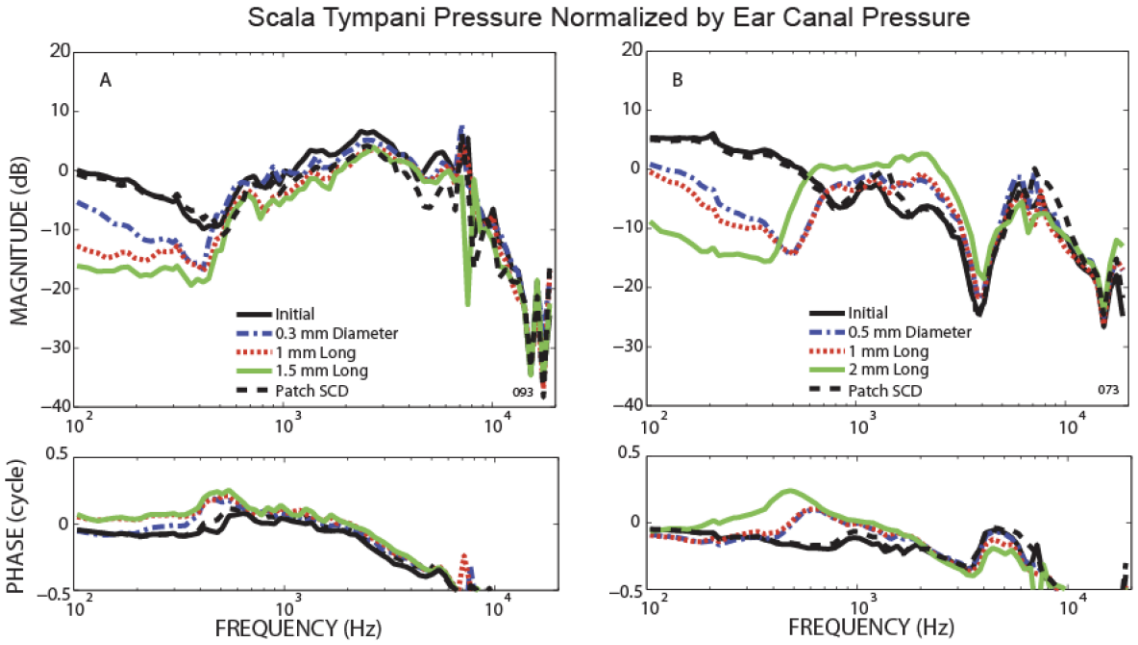

Figure 4.

Representative example of scala tympani pressure relative to ear canal pressure for the initial state, after various SCD sizes, and after patching the SCD.

NIH-PA Author Manuscript

NIH-PA Author Manuscript

NIH-PA Author Manuscript

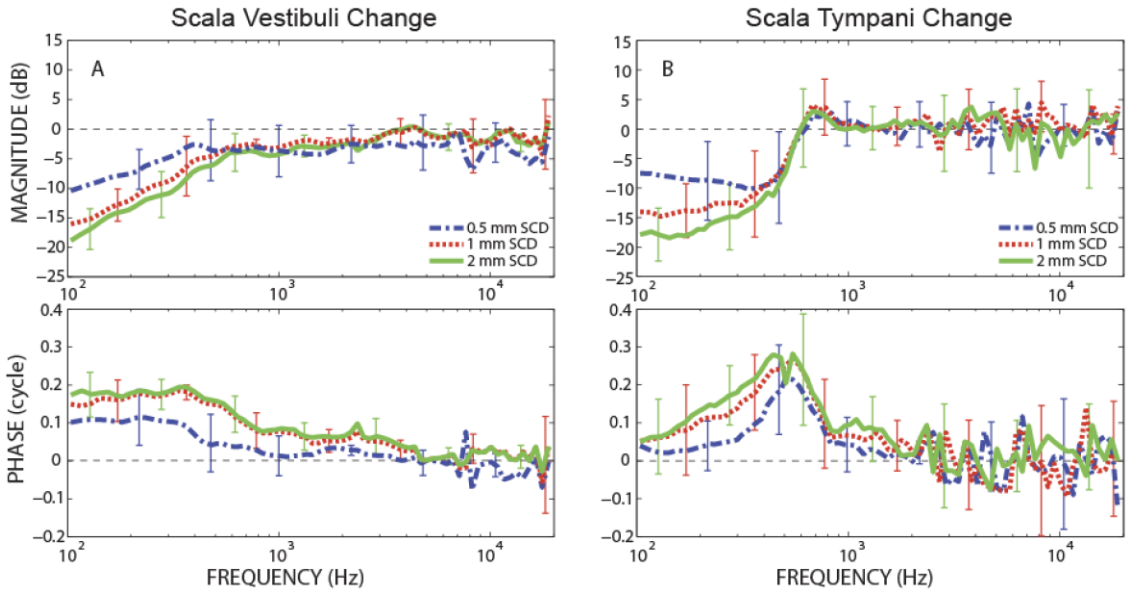

Figure 5.

Changes in scala pressures due to various sizes of SCD, represented with geometric mean and standard deviation (error bars) for magnitudes and linear mean and deviations for phase. (A) Change in P_{SV} (N=5), (B) Change in P_{ST} (N=6).

NIH-PA Author Manuscript
NIH-PA Author Manuscript
NIH-PA Author Manuscript

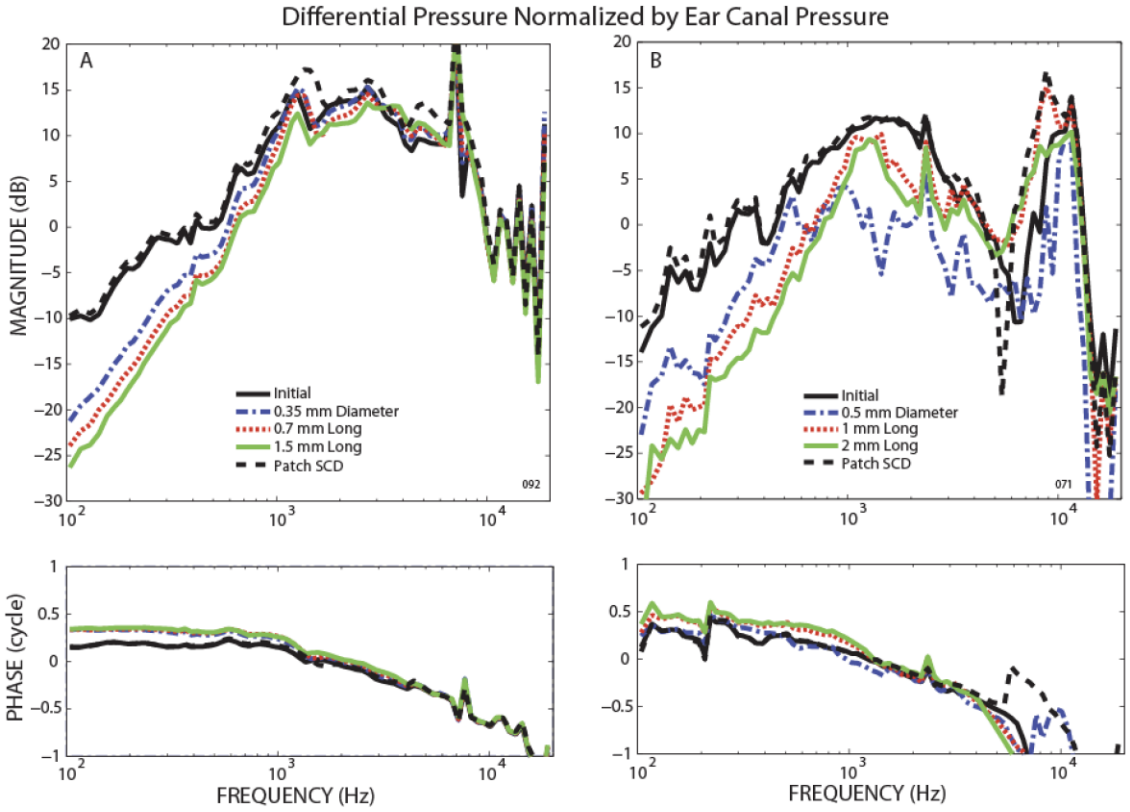

Figure 6.

Representative examples of the differential pressure across the cochlear partition relative to ear canal pressure, $(P_{SV} - P_{ST})/ P_{EC}$, for the initial state, after various SCD sizes, and after patching the SCD.

NIH-PA Author Manuscript NIH-PA Author Manuscript NIH-PA Author Manuscript

Table I

Summary of Specimens

Number	Comment Complication	SV sensor Stable	ST sensor stable	P_{SV} SCD reversed	P_{ST} SCD reversed	V_{stap} SCD reversed
1 (036)	Development					
2 (038)	Development					
3 (047)	Development					
4 (067)	Air					
5 (069)	Low V_{Stap}					
6 (071)		X	X	X	X	X
7 (073)			X		X	X
8 (075)	Trauma					
9 (076)		X	X	X		X
10 (078)	Air					
11 (079)		X	X			X
12 (080)	Air					
13 (081)			X		X	X
14 (082)		X		X		X
15 (083)						
16 (084)	Air					
17 (085)			X		X	X
18 (086)						
19 (087)	Low V_{Stap}					
20 (088)						
21 (089)	Trauma					
22 (090)	Low V_{Stap}					
23 (091)						
24 (092)		X	X	X	X	X
25 (093)		X	X	X	X	X